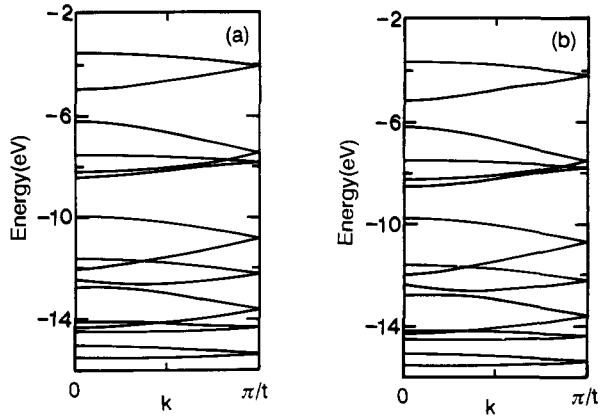

Figure 14. Extended Hückel π-band structure of PTL(II) at (a) q = 1.6 e and (b) q = -1.6 e. Symmetries are same as those for PTL(I) in Figure 6.

bonds and two types of carbon rings. Since these are 2-fold degenerate, solitons can be expected as defects in the neutral form and at low doping levels. The electronic structures of these ladder polymers show two types of bandgaps; small gaps at the Brillouin zone edge arise from the Peierls distortion and large gaps at the center of the Brillouin zone, which are due to the perturbation of the heteroatoms in the chain. The bandgap at the Fermi level originates from Peierls distortion and is small, 0.3–0.5 eV, which may reflect the experimentally observed substantial conductivity of undoped pristine P'TL. The heteroatoms lead to band separations into several narrow bands. Therefore, short carrier delocalization lengths in the heterocyclic ladder polymers, as observed from ^{14}N ENDOR measurements,[7] can be explained by the narrow bandwidth of the uppermost valence band. At around ±0.8 e CT/unit cell, the ladder polymers become highly symmetric and consequently, the bandgaps at the Brillouin zone edge become closed. However, bandgaps due to perturbation of heteroatoms still remain fundamentally unchanged, even up to CT of ±1.6 e/unit cell. This effect may be responsible for the experimental observations that there is only a small increase in conductivity and spin concentrations in doped PTL. An entirely different kind of ladder polymer, BBL (benzimidazobenzophenanthroline-type ladder polymer) will be investigated in a forthcoming publication.[26]

Acknowledgment. Work at Georgetown University was supported by the U.S. Air Force Office of Scientific Research under Grant No. AFOSR-89-0229.

(26) Hong, S. Y.; Kertesz, M.; Lee; Y. S.; Kim, O.-K., to be published.

Tin–Sulfur and Tin–Selenium Phenylated Ring Systems as Organometallic Precursors to Tin Sulfide and Tin Selenide

Steven R. Bahr, Philip Boudjouk,* and Gregory J. McCarthy

Department of Chemistry, North Dakota State University, Fargo, North Dakota 58105

Received September 17, 1991. Revised Manuscript Received November 26, 1991

Group 14–16 six-membered rings, $(Ph_2EX)_3$ (E = Si, Sn; X = S, Se), were synthesized in 49–61% yield from Ph_2ECl_2 and anhydrous Na_2X made from elemental Na and X with a catalytic amount of naphthalene in THF. Pyrolysis of the tin-containing rings, $(Ph_2SnS)_3$ and $(Ph_2SnSe)_3$, at temperatures over 300 °C in a helium atmosphere yielded microcrystalline black powders identified as SnS or SnSe by X-ray diffraction. Scanning electron micrographs show the powders to consist of agglomerates of crystals having platey (SnS) or prismatic (SnSe) habits.

Introduction

Progress in the synthesis of group 13–15 semiconductors, such as GaAs and InP, by organometallic chemical vapor deposition (OMCVD) of single-source precursors[1] has prompted an extension of the technique to prepare group 14–16 analogues as well. Pyrolysis of compounds of the type $R_kE_lX_mR'_n$ (R, R' = C_{1-4} alkyl groups; E = group 14; X = group 16; k = 0–6; l = 1–2; m = 1–4; n = 0–4)[2] or metal selenolates, $[R_2NC(Z)Se]_nM^{n+}$ or $[ROC(Z)Se]_nM^{n+}$ (R = C_{1-10} alkyl group; M = metals; Z = O, Se; n = 1–5),[3] at 250–450 °C gave composite metal sulfides and selenides useful for semiconductor devices and solar cells.

The traditional synthetic approach toward group 14–16 semiconductors through utilization of the OMCVD process involves mixing a tetraalkyl group 14 compound with H_2S or H_2Se (e.g., eq 1).[4] Single-source precursors offer some

$$Me_4Sn + H_2S \xrightarrow[625\ °C]{} SnS + CH_4 + ... \quad (1)$$

important advantages over the traditional methods. These advantages include increased stability toward air and moisture and better hydrocarbon solubility. For the most part, the single-source precursors studied thus far possess small alkyl groups which depart when heated. Compounds with aryl substituents have largely been ignored.

We have begun an investigation in which organometallic systems containing aryl groups are employed to produce potential semiconducting compounds by OMCVD or condensed phase pyrolysis. The most common methods used to synthesize binary compounds by a solid-state approach are sintering the elements at high temperatures and long reaction times[5] and by mixing an alkali-metal chalcogenide

(1) Cowley, A. H.; Jones, R. A. *Angew. Chem., Int. Ed. Engl.* **1989**, *28*, 1208 and references therein.
(2) Domrachev, G. A.; Khamylov, V. K.; Bochkarev, M. N.; Zhuk, B. V.; Kaverin, B. S.; Nesterov, B. A.; Kirillov, A. I. German Patent 2,703,873, 1977.
(3) Uchida, H. Japanese Patent 01,298,010, 1989.
(4) Manasevit, H. M.; Simpson, W. I. *J. Electrochem. Soc.* **1975**, *122*, 444.

0897-4756/92/2804-0383$03.00/0

and a metal halide in aqueous solution.[6] In this paper we describe a new synthesis for phenylated six-membered ring systems, $(Ph_2EX)_3$ (E = Si, Sn; X = S, Se), and the ability of the tin-containing rings to yield SnS or SnSe via solid-state pyrolysis when heated over 300 °C in an inert atmosphere.

Experimental Section

General Procedures. All reagents were purchased from Aldrich except where noted. Sodium sulfide and sodium selenide were prepared from elemental sulfur or selenium and sodium chips cut from pellets. Ph_2SiCl_2 (Petrarch) was distilled, and Ph_2SnCl_2 was used as received. Air-sensitive reagents were transferred in an argon-filled glovebox, and all reactions were performed under a nitrogen atmosphere. Tetrahydrofuran (THF) was distilled from sodium/benzophenone ketyl just prior to use. Benzene was stirred over concentrated H_2SO_4 and distilled from CaH_2. The first 10% fraction collected was discarded. Hexane was stirred over concentrated H_2SO_4 and distilled. Atomic absorption and combustion analyses were performed at Galbraith Laboratories, Knoxville, TN, or Desert Analytics, Tucson, AZ.

Pyrolysis experiments were performed using a Lindberg tube furance 36 cm long with a 3-cm diameter and a 55 × 2.5 cm quartz tube placed inside. One end of the tube was fitted with a one-holed rubber stopper for He gas input, and a liquid N_2 trap connected to a silicone oil bubbler to monitor the He flow rate set at 50 mL/min was attached to the exit end. The sample to be heated was placed in a ceramic crucible (12-mm height × 10-mm diameter).

The ^1H (399.78 MHz), ^{13}C (100.52 MHz), ^{29}Si (79.43 MHz), ^{119}Sn (148.99 MHz), and ^{77}Se (76.22 MHz) NMR spectra were obtained on a JEOL GSX400 spectrometer. A 5-mm broadband probe equipped with a variable-temperature accessory controlled the temperature at 25 ± 0.5 °C. Typical samples were prepared 0.05–0.15 M in $CDCl_3$. ^1H, ^{13}C, and ^{29}Si NMR chemical shifts are reported in parts per million (ppm) with respect to Me_4Si (0 ppm). ^{77}Se NMR shifts are reported with respect to a 25% solution of Me_2Se in $CDCl_3$ (0 ppm), while ^{119}Sn shifts are relative to Me_4Sn in $CDCl_3$ (0 ppm). ^{29}Si NMR spectra were acquired by using a refocused INEPT pulse sequence. Infrared spectra were recorded on a Mattson 2020 Galaxy FT-IR instrument. Gas chromatographic analysis were performed on a cross-linked methylsilicone capillary column. Gas chromatograph/mass spectrometer (GC-MS) and solid sample MS data were obtained on a Hewlett-Packard 5988A GC-MS system equipped with a methyl silicone capillary column. Melting points were taken on a Thomas-Hoover capillary melting point apparatus and are uncorrected.

Scanning electron microscopy (SEM) was performed on a JEOL Model JSM 35 instrument. The SEM samples were sputtered with Au to reduce charging effects. X-ray powder diffraction (XRD) patterns were recorded from ethanol slurry mounted samples on glass slides using a Philips automated diffractometer with Cu Kα radiation and data reduction software from MDI, Inc. The diffractometer was calibrated with a NIST SRM 6406 silicon standard.

Synthesis of $(Ph_2SnSe)_3$ (4). A 100-mL three-neck flask fitted with a condenser/N_2 inlet and a 50-mL addition funnel was charged with sodium chips (1.02 g, 44.0 mmol), selenium powder (1.73 g, 22.0 mmol), naphthalene (0.56 g, 4.4 mmol), and 30 mL THF. To ensure complete consumption of sodium metal, the mixture was refluxed for at least 10 h yielding a white suspension of Na_2Se. (If a purple color persists at this point, small amounts of sodium can be added until a white endpoint is attained. For a green mixture, adding Se powder will eventually give the white mixture.) The Ph_2SnCl_2 (7.6 g, 22 mmol) dissolved in 30 mL of THF was transferred by syringe to the addition funnel and added dropwise to the Na_2Se suspension over 30 min at room temperature. After stirring an additional 2 h, the contents were refluxed for 36 h, producing a gray mixture. This was poured into 75 mL of water followed by saturation with NaCl and extraction with four 50-mL portions of ether. The ether fractions were combined and dried over $MgSO_4$, and the solvent was removed by rotary evaporator, leaving a yellow residue. A hexane rinse to remove the naphthalene and recrystallization in benzene/hexane gave 4.5 g (56% yield) of very light yellow crystals of $(Ph_2SnSe)_3$ (4): mp 176–177 °C (lit.[7] 176–177 °C). An additional recrystallization gave colorless 4 for pyrolysis use. ^{119}Sn NMR ($CDCl_3$) δ −43.5 (lit.[8] δ −44). ^{77}Se NMR ($CDCl_3$) δ −452.

$(Ph_2SnS)_3$ (3). In a 100-mL two-neck flask fitted with a condenser/N_2 inlet and 50-mL addition funnel were placed sodium chips (1.38 g, 60.0 mmol), sulfur powder (0.97 g, 30 mmol), naphthalene (0.80 g, 0.6 mmol), and 30 mL of THF. Stirring at reflux for 12 h left a light yellow suspension. The mixture was cooled to 0 °C, and Ph_2SnCl_2 (10.3 g, 30.0 mmol) dissolved in 20 mL of THF was added dropwise from the addition funnel over 30 min. Stirring was continued for 2 days at room temperature, producing a gray mixture. Aqueous workup and recrystallization from benzene/hexane gave 5.6 g (61% yield) of white crystalline (3): mp 180–183 °C (lit.[9] 183–184 °C). ^{119}Sn NMR ($CDCl_3$) δ 17.6 (lit.[9] δ 16.8).

$(Ph_2SiS)_3$ (1). Na_2S was made on the same scale as for 3, cooled to 0 °C, and treated with a solution of Ph_2SiCl_2 (7.6 g, 30 mmol) in 20 mL of THF over 30 min. Two days of stirring at room temperature produced a tan suspension. The THF was removed by vacuum, 50 mL of benzene was then added, and the mixture was filtered under N_2 to give a yellow solution. A light yellow solid remained after removal of the benzene and rinsing with 10 mL of hexane. Recrystallization from benzene/hexane gave 4.0 g (63% yield) of white, crystalline 1: mp 184–187 °C (lit.[10] 186–188 °C). ^{29}Si NMR ($CDCl_3$) δ 4.44.

$(Ph_2SiSe)_3$ (2). A procedure similar to that for 1 gave a 49% yield of white, crystalline 2: mp 194–197 °C (lit.[11] 195–197 °C). ^{29}Si NMR ($CDCl_3$) δ 3.70 (lit.[11] δ 3.70). ^{77}Se NMR ($CDCl_3$) δ −287 (lit.[11] δ −287).

Pyrolysis of $(Ph_2SnS)_3$ (3). The pyrolysis of $(Ph_2SnS)_3$ (3) described below is typical of all ring systems. $(Ph_2SnS)_3$ (0.433 g, 0.473 mmol) was weighed in a ceramic crucible and placed in a quartz tube furnace set at 200 °C. The tube was thoroughly flushed with He, and then the temperature was raised to 450 °C over 1 h and held there for an additional 1 h before cooling to room temperature. A black powder, identified as orthorhombic SnS by its X-ray powder diffraction pattern and atomic absorption analysis, remained in the crucible (145 mg, 33%). A clear, colorless crystalline solid (260 mg) with some yellowish oil was isolated from the end of the quartz tube and liquid N_2 trap to give 94% total mass recovery. GC analysis of a solution (CH_2Cl_2) of the solid and the oil showed two products. The clear, crystalline solid was identified as Ph_4Sn (41% GC yield): mp 223–225 °C (lit.[12] 225–226 °C). ^{119}Sn NMR ($CDCl_3$) δ −129 (lit.[13] δ −128.1). The other product was identified as Ph_2S (18% GC yield) by comparison of GC-MS and ^{13}C NMR data with an authentic sample. The SnS could be sublimed at 900 °C in the same pyrolysis apparatus to give shiny, platelike crystals which formed on the walls of the quartz tube as it exited the furnace. Combustion analysis found approximately 0.05% carbon.

Pyrolysis of $(Ph_2SnSe)_3$ (4). 4 (0.395 g, 0.374 mmol) was pyrolyzed giving 144 mg of SnSe identified by atomic absorption analysis and its X-ray powder diffraction pattern. The volatile trapped products (240 mg, 97% total recovery) contained three compounds of which one was Ph_4Sn (37% yield). Ph_2Se (18% yield) was identified by comparison of GC-MS and ^{13}C NMR data with an authentic sample. A small amount of $Ph_3SnSePh$ (<5% GC yield) was detected. ^{119}Sn NMR ($CDCl_3$) δ −79 (lit.[14] δ −79.2).

(5) Yellin, N.; Ben-Dor, L. *Mater. Res. Bull.* **1983**, *18*, 823.
(6) Korczynski, A.; Lubomirska, I.; Sobierajski, T. *Chem. Stosow.* **1981**, *25*, 391.
(7) Schumann, H.; Thom, K. F.; Schmidt, M. *J. Organomet. Chem.* **1964**, *2*, 361.
(8) Furue, K.; Kimura, T.; Yasuoka, N.; Kasai, N.; Kakudo, M. *Bull. Chem. Soc. Jpn.* **1970**, *43*, 1661.
(9) Schmidt, M.; Dersin, H.-J.; Schumann, H. *Chem. Ber.* **1962**, *95*, 1428.
(10) Mayfield, D. L.; Flath, R. A.; Best, L. R. *J. Org. Chem.* **1964**, *29*, 2444.
(11) Boudjouk, P.; Bahr, S. R.; Thompson, D. P. *Organometallics* **1991**, *10*, 778.
(12) Chambers, R. F.; Scherer, P. C. *J. Am. Chem. Soc.* **1926**, *48*, 1054.
(13) Holecek, J.; Nadvornik, M.; Handlir, K.; Lycka, A. *J. Organomet. Chem.* **1983**, *241*, 177.

Scheme I. Synthesis of Group 14–16 Rings

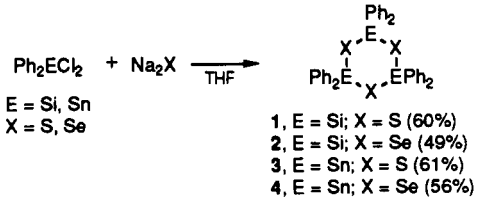

Table I. Atomic Absorption and Combustion Analyses for SnX Powders

compd pyrolyzed	wt % Sn[a]	wt % X[a]	wt % C
$(Ph_2SnS)_3$	79.33 ± 0.6 (78.73)	21.31 ± 0.1 (21.27)	0.14 ± 0.1
$(Ph_2SnSe)_3$	60.65 ± 1.0 (60.05)	39.40 ± 0.8 (39.95)	0.35 ± 0.1

[a] Calculated percentage for SnX in parentheses.

^{77}Se NMR ($CDCl_3$) δ −20.1. MS: m/e 429 (Ph_3SnSe^+, 3.5%); 351 (Ph_2SnSe^+, 100%) with both of the listed peaks having the correct isotope distribution for one Sn and one Se atom in the surrounding region.

Results and Discussion

Synthesis and Characterization of $(Ph_2EX)_3$ Rings. Recently we reported procedures for making anhydrous sodium sulfide[15] and sodium selenide[16] by combining sodium, sulfur, or selenium and a catalytic amount of naphthalene in THF. When either Ph_2SiCl_2 or Ph_2SnCl_2 was added to Na_2S or Na_2Se, six-membered rings of the formula $(Ph_2EX)_3$ (E = Si, Sn; X = S, Se) were isolated (Scheme I). Commercially available Na_2S or Na_2Se under these reaction conditions typically gave very poor results (<10% yield). This method gives yields of compounds 1–4 comparable to those previously reported (see Experimental Section). All of these compounds are white solids which crystallize easily from benzene/hexane solutions. Compounds 3 and 4 are stable for weeks in air. However, 1 and 2 are slightly moisture sensitive, resulting in some decomposition after several hours.

Pyrolysis of Tin-Containing Ring Systems. Solid-state pyrolysis studies were conducted under a slow flow of helium gas at atmospheric pressure. $(Ph_2SnS)_3$ (3) and $(Ph_2SnSe)_3$ (4) undergo decomposition above 300 °C depositing a black or dark gray powder in the crucible. These dark powders were identified as having the approximate formula SnX by atomic absorption (Sn, Se) or combustion analysis (S; Table I). Analyses obtained for SnS were typically closer to the calculated values than those determined for SnSe. Combustion analysis also showed a lower percentage of residual carbon impurity for SnS. Since infrared analysis of the powders did not reveal the presence of aromatic C–H stretching bands, it is unknown whether the carbon impurity arises from elemental carbon or phenylated compounds. Sublimation of the SnS powder in the same pyrolysis apparatus gave shiny, metallic-looking flat crystals having approximately 0.05% carbon impurity as determined by combustion analysis. $(Ph_2SiS)_3$ (1) and $(Ph_2SiSe)_3$ (2) underwent sublimation along with some decomposition but very little residue remained in the crucible. For this reason, the pyrolysis results of 1 and 2 were not pursued further.

Predominantly two volatile products are formed during the pyrolysis of $(Ph_2SnS)_3$ (3) and $(Ph_2SnSe)_3$ (4). Overall, at least 94% of the weight could be recovered in the form of SnX and volatile products. The yields of Ph_2X and Ph_4Sn were determined by GC relative to an added amount of dodecane as an internal standard (Table II). These yields are close to theoretical for eq 2 (Table II). In the pyrolysis of 4, a small amount (<5%) of $Ph_3SnSePh$ was identified by GC-MS and the ^{119}Sn NMR resonance in $CDCl_3$ at −79.0 ppm (lit.[12] δ −79.2). It is noteworthy that no biphenyl was identified in any of the pyrolysis reactions, suggesting that phenyl radicals do not play an important role in the mechanism. One plausible reaction pathway involving several intramolecular phenyl migrations is consistent with the simplicity of the product distribution (Scheme II). Since the reaction occurs when 3 or 4 is a neat liquid in the crucible, a similar mechanism involving intermolecular phenyl migrations cannot be ruled out at this time. A radical mechanism can also be envisioned where tin and chalcogen radicals exist since free-radical migration of aryl groups is common in organic systems.[17] Both mechanisms resemble the process of redistribution known to occur in many organotin systems.[18] It appears the phenyl groups serve two purposes: (1) to provide enough weight on the molecule to prevent sublimation

Table II. Pyrolysis Results of $(Ph_2SnX)_3$ Rings

$$(Ph_2SnX)_3 \xrightarrow[450\ °C]{He,\ 1\ atm} \underset{A}{2SnX} + \underset{B}{Ph_2X} + \underset{C}{Ph_4Sn} + \underset{D}{Ph_3SnXPh} \quad (2)$$

compd pyrolyzed	% yields[a] A	B[b]	C[b]	D[b]	total mass recovery
$(Ph_2SnS)_3$	33 (33)	18 (20)	41 (47)	0 (0)	94
$(Ph_2SnSe)_3$	36 (37)	18 (22)	37 (40)	<5 (0)	97

[a] Theoretical yield is in parentheses assuming the production of only A, B, and C. [b] Yield determined by GC.

Table III. XRD Measured Unit Cell Parameters for SnS[a]

referenced work	a, Å	b, Å	c, Å	vol, Å^3
PDF 33-1375	4.3340	11.2000	3.9870	193.53
PDF 39-354	4.3291 (2)	11.1923 (4)	3.9838 (2)	193.03
DelBucchia et al.[19]	4.329	11.180	3.982	192.72
Mosburg et al.[20]	4.328	11.190	3.987	193.09
this study	4.3184 (12)	11.185 (2)	3.9848 (12)	192.48 (06)

[a] SnS, orthorhombic [GeS] structure type, space group *Pbnm*, Z = 4.

Scheme II. Proposed Mechanism for Pyrolysis of $(Ph_2SnX)_3$

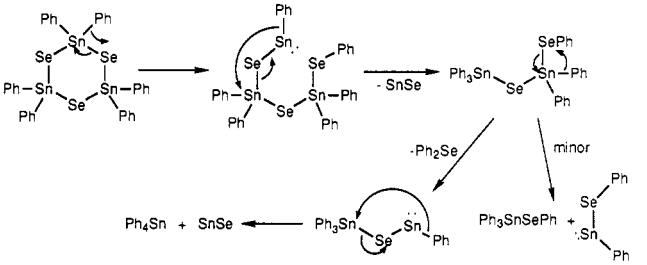

(14) Jones, C. H. W.; Sharma, R. D.; Taneja, S. P. *Can. J. Chem.* **1986**, *64*, 988.
(15) So, J.-H.; Boudjouk, P. *Synthesis* **1989**, 306.
(16) Thompson, D. P.; Boudjouk, P. *J. Org. Chem.* **1988**, *53*, 2109.
(17) March, J. *Advanced Organic Chemistry*, 3rd ed.; Wiley: New York, 1985; p. 955 and references therein.
(18) Armitage, D. A. In *Comprehensive Organometallic Chemistry*; Wilkinson, G., Stone, F. G. A., Abel, E. W., Eds.; Pergamon Press: Oxford, England, 1982; Vol. 2, Chapter 11.
(19) DelBucchia, P. S.; Jumas, J.-C.; Maurin, M. *Acta Crystallogr.* **1981**, *B37*, 1903.
(20) Mosburg, S.; Ross, D. R.; Bethke, M.; Toulmin, P. *U.S. Geol. Surv., Profess. Papers* **1961**, *424-C*, 347.
(21) Okazaki, A.; Ueda, I. *J. Phys. Soc. Jpn.* **1956**, *11*, 470.
(22) Nesterova, Y. M.; Pashinkin, A. S.; Novoselov, A. V. *Russ. J. Inorg. Chem.* **1961**, *6*, 1031.
(23) Weidemeier, H.; Csillag, F. *Z. Kristallogr.* **1979**, *149*, 17.

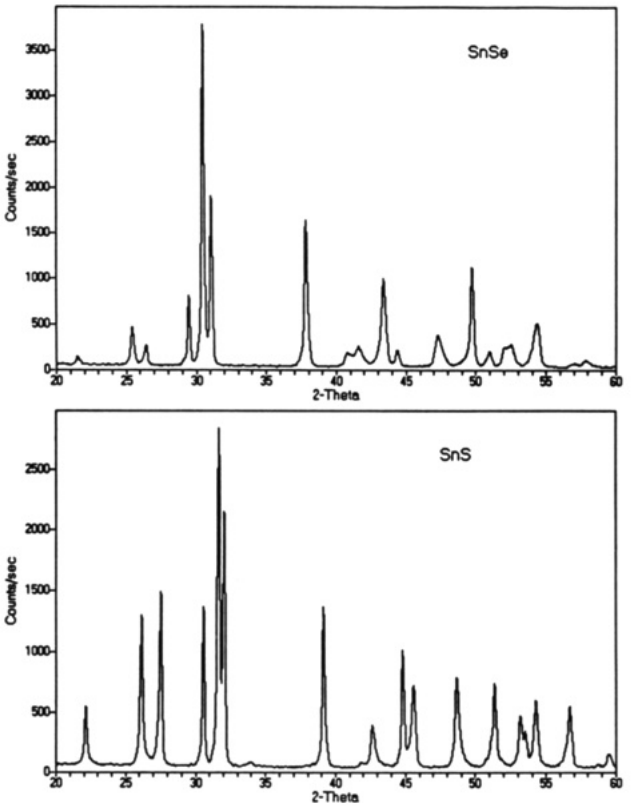

Figure 1. X-ray diffraction patterns (Cu Kα) for SnS obtained from the pyrolysis of $(Ph_2SnS)_3$ at 450 °C and of SnSe from pyrolysis of $(Ph_2SnSe)_3$ at 450 °C.

before decomposition occurs; (2) to serve as a good migrating group during the redistribution process.

X-ray Diffraction (XRD) Analysis of SnX Powders. The X-ray diffractograms of SnS (Figure 1) were in very good agreement with the observed (39–354) and calculated (33–1375) reference patterns in Set 40 of the ICDD Powder Diffraction File (PDF). Unit cell parameters, obtained from the measured peaks (corrected with the external diffractometer standard) using a least-squares unit cell parameter refinement, compared well with the values given in the PDF and other sources, although the cell was slightly smaller than the range of those previously reported (Table III). SnS was phase pure, i.e., there were no extraneous peaks of carbon or any other phases in the diffractograms.

The isostructural SnSe was also phase pure and in fair agreement in peak positions and intensities with PDF 32-1382, a calculated pattern of SnSe. However, there were minor peak shifts between the two patterns. A comparison of the refined unit cell parameters with other sources of SnSe cells shows that the *a* cell parameter is somewhat smaller, but the *b* and *c* parameters are within the range of the reported values (Table IV). The differences in the cell parameters between the PDF pattern and those determined in this study explain the peak shifts noted in Table IV.

Neither of the SnX diffractograms resolved the Cu $K\alpha_1/\alpha_2$ doublet, and the peaks profiles were broad, with those of the selenide being broader than the sulfide. Specifically, the strongest peaks of SnS and SnSe had full width at half-maximum values of 0.16° and 0.20°, respectively, compared to an instrument profile of 0.11° for a well-ordered stoichiometric material (NIST SRM 660 LaB_6). These observations suggest small crystallite size or only moderate crystalline order, perhaps due to some slight nonstoichiometry or stoichiometry range. There could also be some broadening due to strain introduced in sample preparation.

Scanning Electron Microcropy of SnX. SEM photographs for SnS powder produced from the pyrolysis of $(Ph_2SnS)_3$ at 450 °C are shown in Figure 2. The particles appear as microcrystalline rosette clusters predominantly in the 1-μm size range with some clusters 3–5 μm. Thickness of the individual petals is 250–500 Å, which is also roughly the step size of the contours shown in Figure 3 for a SnS crystal grown by sublimation of the powder

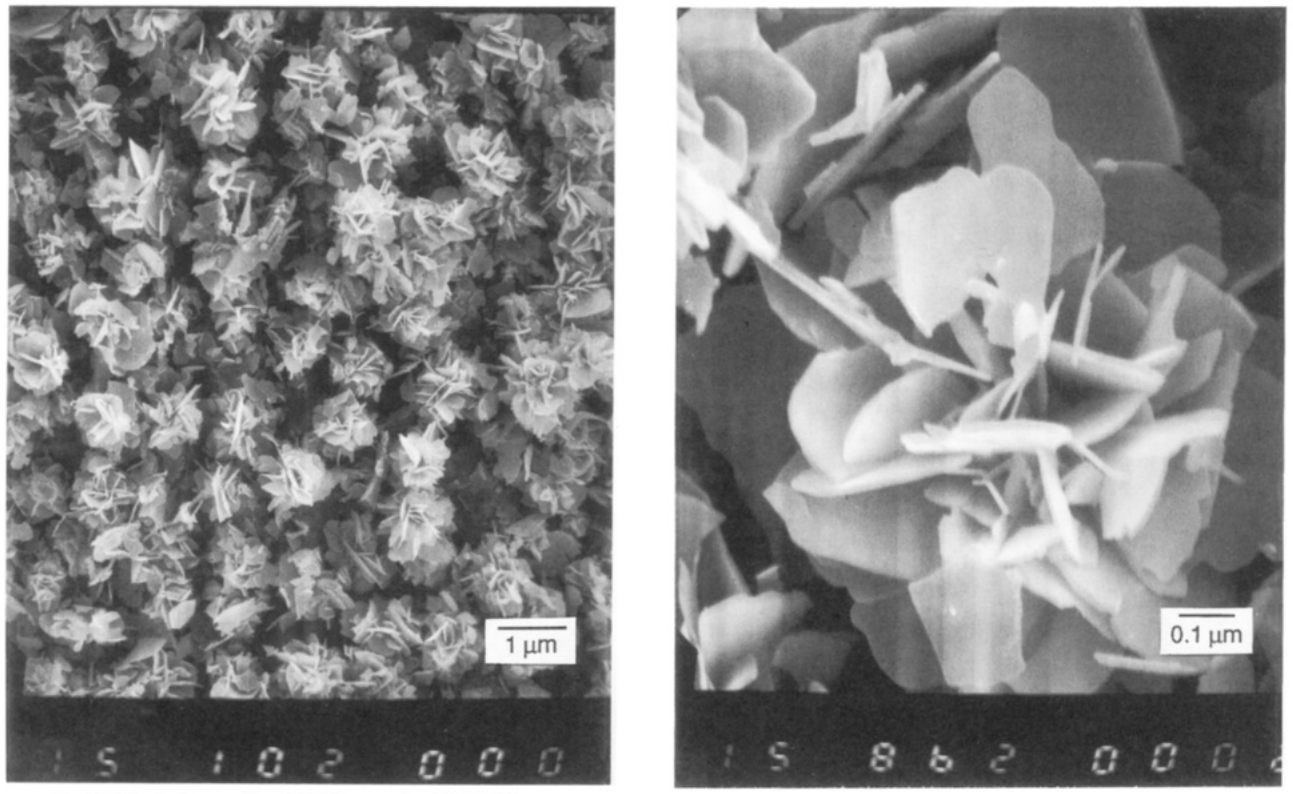

Figure 2. SEM photographs of SnS powder (15 kV).

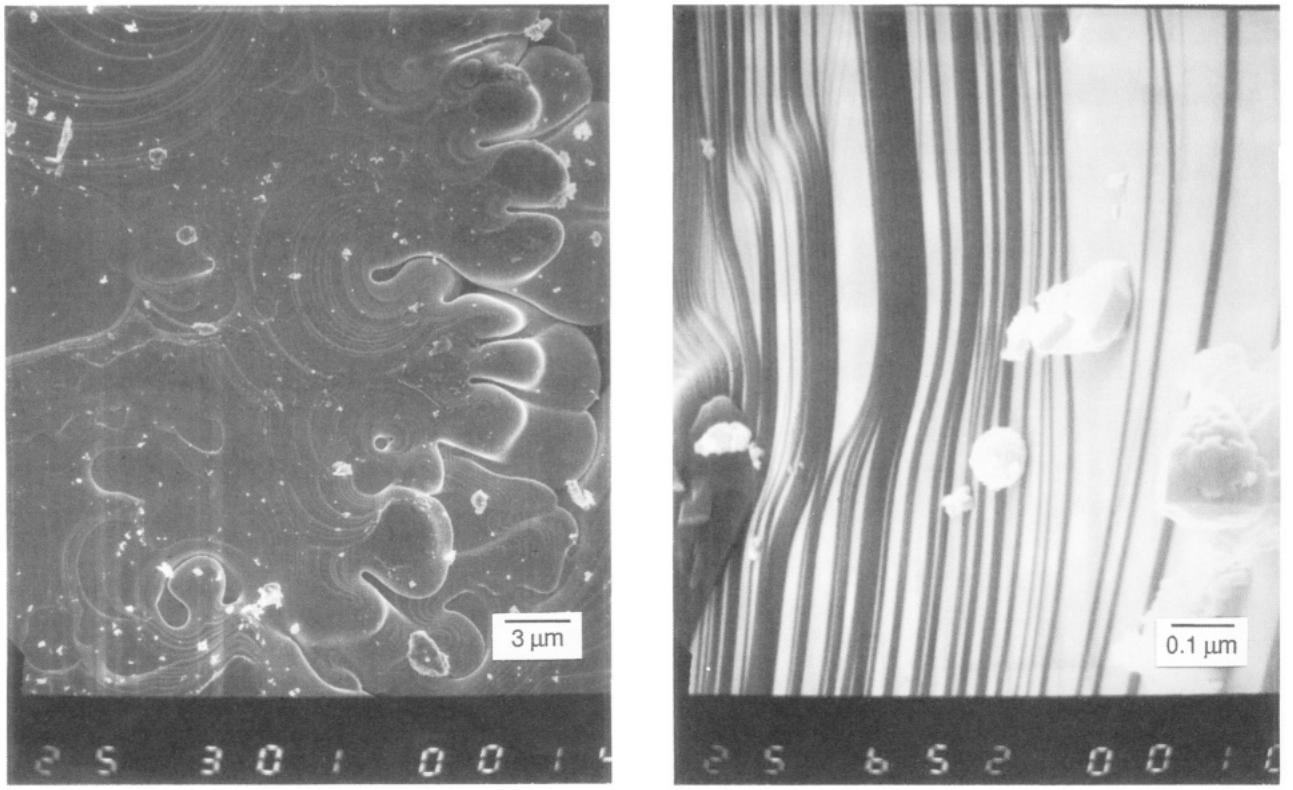

Figure 3. SEM photographs of the surface of a SnS crystal formed by sublimation of powder at 900 °C (30 kV).

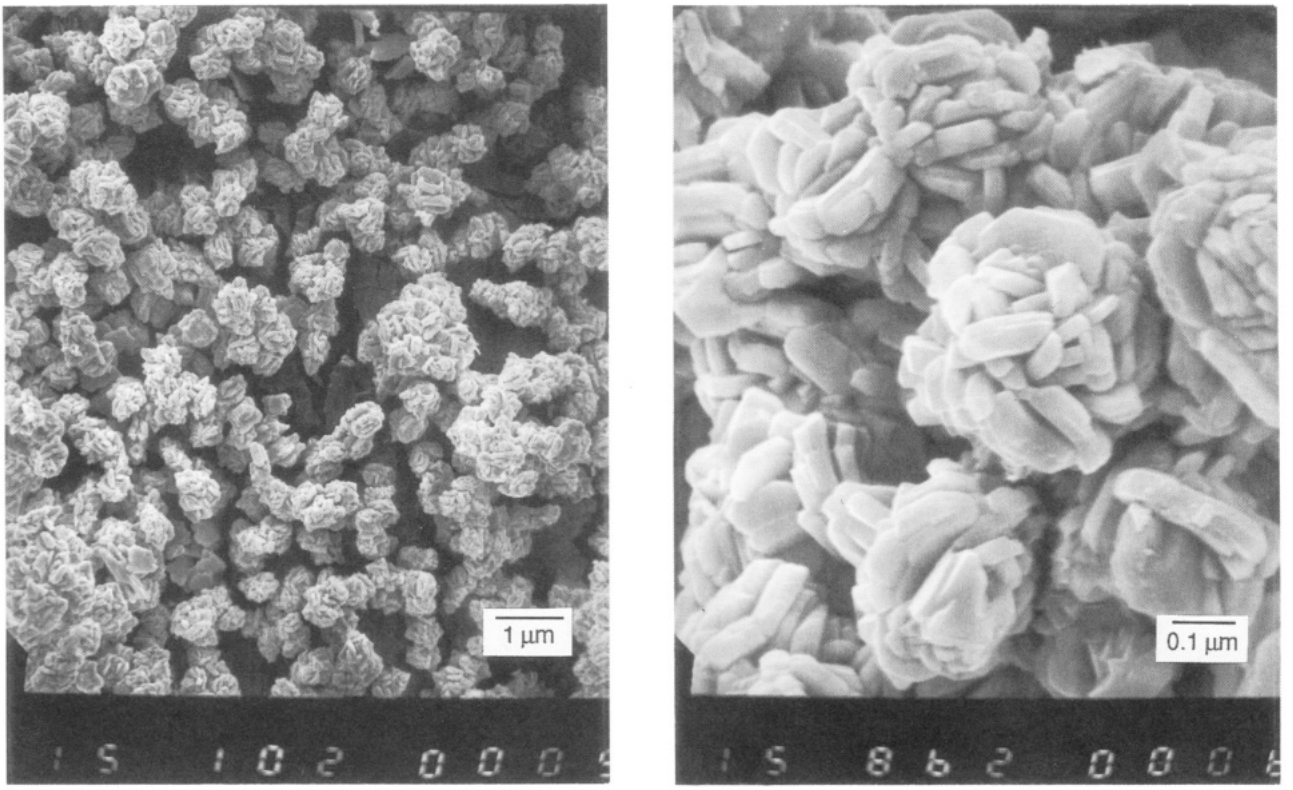

Figure 4. SEM photographs of SnSe powder (15 kV).

Table IV. XRD Measured Unit Cell Parameters for SnSe

referenced work	*a*, Å	*b*, Å	*c*, Å	vol, Å^3
PDF 32-1382	4.46	11.42	4.19	213.4
Okazaki et al.[21]	4.46	11.57	4.19	216.2
Nesterova et al.[22]	4.47	11.48	4.19	215.0
Wiedemeier et al.[23]	4.445	11.501	4.153	212.31
this study	4.418 (1)	11.515 (7)	4.170 (1)	212.19 (14)

[a] SnSe, orthorhombic [GeS] structure type, space group *Pbnm*, $Z = 4$.

at 900 °C. The SnSe powder showed a prismatic rather than tabular habit (Figure 4). The SnSe particles are not as uniform as those of SnS but rather exist as 1–10-μm clusters of crystals which are approximately 0.2–0.4 μm by about 0.05 μm in size.

Conclusions

$(Ph_2SnS)_3$ and $(Ph_2SnSe)_3$ offer several advantages as organometallic solid-state precursors to SnS and SnSe.

Among these are ease of synthesis and purification, high stability toward air and moisture, and their ability to generate microcrystalline SnS and SnSe powders cleanly and conveniently by simple heating to 450 °C under a helium atmosphere.

Acknowledgment. Financial support from the Air Force Office of Scientific Research through Grants 88-0060 and 91-0197 and Dow Corning Corp. is gratefully acknowledged. We also thank Jody Solem and Jason Bender for their help in aquiring XRD patterns and Dr. Thomas Freeman for obtaining SEM photographs.

Registry No. 1, 15287-09-9; 2, 132776-76-2; 3, 16892-66-3; 4, 105860-17-1; Ph_2SnCl_2, 1135-99-5; Ph_2SiCl_2, 80-10-4; SnS, 1314-95-0; Ph_4Sn, 595-90-4; Ph_2S, 139-66-2; SnSe, 1315-06-6; Ph_2Se, 1132-39-4; $Ph_3SnSePh$, 29328-48-1.

Preparation, Ionic Conductivity, and Humidity-Sensing Property of Novel, Crystalline Microporous Germanates, $Na_3HGe_7O_{16}\cdot xH_2O$, x = 0–6. 1

Shouhua Feng, Menting Tsai, and Martha Greenblatt*

Department of Chemistry, Rutgers, The State University of New Jersey, New Brunswick, New Jersey 08903

Received September 23, 1991. Revised Manuscript Received December 3, 1991

A crystalline microporous germanate, $Na_3HGe_7O_{16}\cdot 6H_2O$, has been hydrothermally synthesized from a Na_2O–GeO_2–H_2O system. This phase undergoes a phase transition to $Na_3HGe_7O_{16}\cdot xH_2O$, x = 0–4 at ~160 °C. Both phases of the sodium germanates have been characterized by powder X-ray diffraction and differential thermal and thermogravimetric analyses. Sodium and proton ionic conductivities in $Na_3HGe_7O_{16}\cdot 6H_2O$, $Na_3HGe_7O_{16}\cdot 4H_2O$, and dehydrated $Na_3HGe_7O_{16}$ were studied by an ac impedance technique. In $Na_3HGe_7O_{16}\cdot 6H_2O$ motion of surface, bulk proton, and Na^+ ion respectively dominate the conductivity in different temperature ranges. The conductivity in dehydrated $Na_3HGe_7O_{16}$ is $\sim 10^{-8}$ $(\Omega\ cm)^{-1}$ at 125 °C and $\sim 10^{-3}$ $(\Omega\ cm)^{-1}$ at 500 °C with an activation energy E_a = 0.64 eV. Humidity-sensing property of $Na_3HGe_7O_{16}\cdot 6H_2O$ and $Na_3HGe_7O_{16}\cdot 4H_2O$ was investigated in the temperature range 50–120 °C.

Introduction

Since the 1950s many investigations of ionic conductivity of crystalline microporous aluminosilicate zeolites have been reported.[1-3] Less information is available on the ionic conductivity of the crystalline microporous germanates, $M_3HGe_7O_{16}\cdot 4$–$6H_2O$, M = Li^+, Na^+, K^+, NH_4^+, Rb^+, and Cs^+. Studies on the X-ray characterization,[4-8] NMR measurements,[9-11] and adsorption properties[12] have been published for germanates and some features of the structure have been determined based on powder X-ray diffraction (PXD) data.[13] The cubic framework structure of the germanates, which is identical to that of the mineral pharmacosiderite,[14] is built up of face- and edge-sharing GeO_6 octahedra which corner share with GeO_4 tetrahedra (Figure 1). In this structure, channels of eight-membered rings with a window size of 4.3 Å lie in the (100) directions connecting cavities in which mobile sodium cations and water molecules are located. This mixed tetrahedral–octahedral framework structure is novel and different from the traditional aluminosilicate zeolites where only TO_4 tetrahedra (T = Si, Al, or Ge) are the basic building units. Mixed TO_6 and TO_4 units are also found in the structures of recently synthesized microporous stannosilicates[15] and gallophosphates.[16,17]

In this paper we report the results of the ionic conductivity and humidity sensing property of the microporous Na–germanates.

Experimental Section

$Na_3HGe_7O_{16}\cdot 6H_2O$ was synthesized under hydrothermal conditions at 150–180 °C in sealed systems containing an aqueous mixture of sodium hydroxide and the α-quartz form of germanium dioxide. A typical synthetic procedure began with the combination of GeO_2 (Eagle-Picher Co., reagent grade) and the aqueous solution of NaOH (Fisher, reagent grade) to form an aqueous gel having molar composition $1.0Na_2O\cdot GeO_2\cdot 80H_2O$. Crystallization of the aqueous gel was carried out in stainless steel autoclaves lined with poly(tetrafluoroethylene) (PTFE) under autogenous pressure at 180 °C for 3 days. The crystalline product ($Na_3HGe_7O_{16}\cdot 6H_2O$) was filtered, washed with

* To whom correspondence should be addressed.

(1) Breck, D. W. *Zeolite Molecular Sieves, Synthesis, Structure and Use*; Wiley: New York, 1974; p 457.
(2) Andersen, E. K.; Andersen, I. G. K.; Skou, E.; Yde-Andersen, S. *Solid State Ionics* **1986**, *18* and *19*, 1170.
(3) Ozin, G. A.; Kuperman, A.; Stein, A. *Angew. Chem., Int. Ed. Engl.* **1989**, *3*, 28.
(4) Zemann, V. J. *Acta Crystallogr.* **1959**, *12*, 252.
(5) Bittner, H.; Kerber, W. *Monatsh. Chem.* **1969**, *100*, 427.
(6) Hauser, E.; Nowotny, H.; Seifert, K. J. *Monatsh. Chem.* **1970**, *101*, 715.
(7) Hauser, E.; Bittner, H.; Nowotny, H. *Monatsh. Chem.* **1970**, *101*, 1864.
(8) Seifert, K. J.; Nowotny, H.; Hauser, E. *Monatsh. Chem.* **1971**, *102*, 1006.
(9) Wada. T.; Cohen-Addad, J. P. *Bull. Soc. Fr. Mineral. Cristallogr.* **1969**, *92*(2), 238.
(10) Bittner, H.; Hauser, E. *Monatsh. Chem.* **1970**, *101*, 1471.
(11) Hauser, E.; Hoch, M. J. R. *J. Magn. Reson.* **1973**, *10*, 211.
(12) Nowotny, H.; Wittmann, A. *Monatsh. Chem.* **1954**, *85*, 558.
(13) Wittmann, A. *Fortschr. Miner.* **1966**, *43*(2), 230.
(14) Wilson, A. J. C., Ed. *Structure Reports*; Oosthoek-Utrecht: The Netherlands, 1947–1948; Vol. 11, p 405.
(15) Corcoran, E. W.; Nawsam, Jr. J. M.; King, Jr. H. E. and Vaughan, D. E. W. *Zeolite Synthesis*; Occelli, M., Robson, H. E., Eds.; 1989; p 603.
(16) Feng, S.; Xu, R.; Yang, G.; Shun, H. *Chem. J. Chinese Univ. (Engl. Ed.)* **1988**, *4* (2), 9.
(17) Wang, T.; Yang, G.; Feng, S.; Shang, C.; Xu, R. *J. Chem. Soc., Chem. Commun.* **1989**, *2436*.

0897-4756/92/2804-0388$03.00/0